

# SUBDOMAIN UNCERTAINTY OPTIMIZATION FOR CROSS-SPEED FAULT DIAGNOSIS

Jianbo Zheng, Lida Huang\*, Tairui Zhang, Bin Jiang, Chao Yang

College of Computer Science and Electronic Engineering  
Hunan University, Changsha, China

## ABSTRACT

Cross-speed bearing fault diagnosis based on unsupervised domain adaptation can handle data distribution differences across various operating speeds, supporting intelligent maintenance of equipment like wind turbines with variable operating speeds. Existing methods focus on aligning sample distributions between source and target domains through global or subdomain correlations. However, these methods overlook essential relationships, such as possible high sample similarity between target subdomains and discrepancies in decision boundaries between source and target domains, leading to substantial class confusion issues. To address class confusion, this paper proposes a subdomain uncertainty optimization method by using these relationships. Class uncertainty is proposed to quantify the degree of classification ambiguity among target domain samples, facilitating the differentiation of high-similarity samples. Boundary optimization is introduced to refine decision boundaries learned from the source domain, alleviating the adverse effects of boundary discrepancies between domains. Additionally, the CL-CNN network is adopted and adjusted to collaborate with the class uncertainty term and boundary optimization term, thus achieving optimal cross-speed fault diagnosis. Extensive experiments conducted across 18 cross-speed tasks demonstrate the superiority of the proposed method, which achieves a stable average accuracy of 99.86%. All code will be released on <https://github.com/IWantBe/SUO>.

**Index Terms**— Unsupervised domain adaptation, cross-speed fault diagnosis, convolutional neural network

## 1. INTRODUCTION

Bearings are essential components in machinery like wind turbines. High-precision and stable bearing fault diagnosis methods are crucial for reducing maintenance costs and minimizing economic losses from equipment failures for manufacturing companies, including wind farms [1, 2]. Currently, significant advancements have been made in deep learning-based bearing fault diagnosis, utilizing vibration data [3, 4, 5, 6]. However, the optimal performance of deep learning methods relies on a consistent sample distribution between training and test data [7]. In practical applications, such as wind turbines, the operating speed of bearings can vary significantly due to dynamic factors like wind forces. This variation can lead to discrepancies in sample distribution and diminish the performance of deep learning methods under cross-speed conditions [8, 9].

Existing unsupervised domain adaptation (UDA) methods facilitate bearing cross-speed fault diagnosis by aligning the sample distributions between a labeled source domain (at one operating speed)

\*This work was supported by the National Natural Science Foundation of China under Grant No.62072169, the China Scholarship Council Program under Grant No.202306130083, and the Postgraduate Scientific Research Innovation Project of Hunan Province under Grant No.QL20230099.

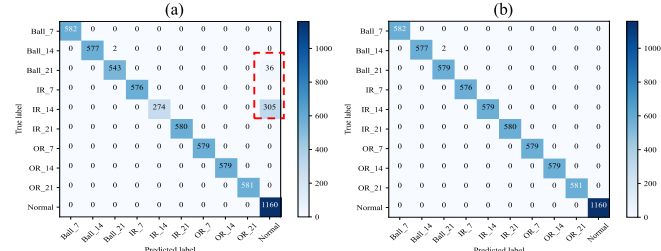


**Fig. 1:** The confusion matrix for cross-speed task 1730→1797 from CWRU. Subfigure (a) presents the confusion matrix of existing method [10], which suffers from significant class confusion issues; numerous samples with the true label IR\_14 and some with Ball\_21 are misclassified as normal. In contrast, subfigure (b) is the confusion matrix under our proposed subdomain uncertainty optimization method, which effectively addresses these class confusion issues.

and an unlabeled target domain (at a different operating speed) [11, 12]. These methods focus on aligning sample distributions between source and target domains by leveraging either global or subdomain correlations, where a subdomain refers to a subset of samples belonging to the same class. Furthermore, they ensure that the decision boundaries learned from the source domain are effectively and directly generalized to the target domain. UDA methods are generally categorized into two types. The first type, based on adversarial learning, employs adversarial neural networks to align global or subdomain distributions [13]. Unfortunately, training these networks is challenging. The second type, which is the focus of this study, utilizes statistical measures such as maximum mean discrepancy (MMD) [14], Multiple Kernel MMD (MK-MMD) [15], Joint MMD (JMMD) [16], CORAL [17], or Local MMD (LMMD) [18, 19, 20, 21] to align global or subdomain distributions.

However, existing UDA methods based on statistical measures encounter significant class confusion (misclassification) issues [22, 23]. Fig. 1 (a), sourced from the existing work [10], presents the confusion matrix for the cross-speed task 1730→1797 from the Case Western Reserve University (CWRU) dataset, which will be detailed in Section 3.1. The confusion matrix illustrates that numerous samples from the IR\_14 category are misclassified as normal, with misclassification rates exceeding 50%. Moreover, some samples from the Ball\_21 category are misclassified as normal, with misclassification rates of 6.22%. These class confusion issues severely undermine model stability and result in suboptimal performance in cross-speed bearing fault diagnosis.

Following the results in Fig. 1 (a), we identify two essential relationships leading to class confusion issues. **(1) High sample similarity between target subdomains.** Samples from different target subdomains may exhibit high similarity, making it challenging for the model to distinguish between them. **(2) Discrepancies in deci-**

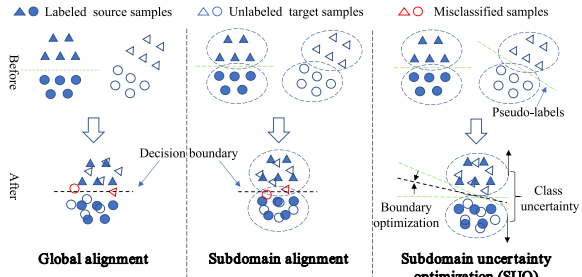


**Fig. 2:** Existing global and subdomain alignment versus our proposed subdomain uncertainty optimization. On the left and in the middle, the global alignment and subdomain alignment methods are depicted. Both methods face challenges with class confusion and contain some misclassified samples. Conversely, on the right, based on subdomain alignment, our subdomain uncertainty optimization SUO method effectively addresses class confusion without introducing misclassified samples. Our SUO method addresses class confusion by integrating the class uncertainty, which facilitates the differentiation of high-similarity samples within target domains, along with the boundary optimization that alleviates discrepancies in decision boundaries between source and target domains.

**sion boundaries between source and target domains.** The decision boundaries learned from the source domain may not be suitable for the target domain, thus causing some samples to be misclassified.

To address class confusion issues, this paper proposes a subdomain uncertainty optimization (SUO) method for cross-speed fault diagnosis. Our SUO method incorporates the subdomain alignment, along with the class uncertainty and boundary optimization, as illustrated in Fig. 2. **The class uncertainty** quantifies the degree of classification ambiguity among target domain samples, aiding in the differentiation of high-similarity samples by minimizing class uncertainty and effectively mitigates class confusion. **The boundary optimization** utilizes high-accuracy pseudo-labels from target domain to refine the decision boundaries learned from the source domain. This refinement enhances the adaptability of these boundaries to target domain samples, further mitigating class confusion. Furthermore, the CL-CNN network [10] is adopted and adjusted to collaborate with the class uncertainty and boundary optimization for optimal cross-speed fault diagnosis.

The results in Fig. 1 (b) have demonstrated the effectiveness of the SUO on the cross-speed task 1730→1797 from CWRU. Extensive experiments conducted on two public datasets, covering 18 cross-speed fault diagnosis tasks, further validate the efficacy of the proposed SUO method with a stable average accuracy of 99.86%.

## 2. THE SUBDOMAIN UNCERTAINTY OPTIMIZATION

We propose the SUO method to address the class confusion issues present in existing methods. This method integrates class uncertainty, which facilitates the differentiation of high-similarity samples within target domains, along with the boundary optimization that alleviates discrepancies in decision boundaries between source and target domains. The framework of the SUO method is illustrated in Fig. 3.

### 2.1. Problem Definition

The unsupervised domain adaptation for cross-speed fault diagnosis task is defined as follows: Given a labeled source domain  $D^s = \{(x_i^s, y_i^s) | i \in [1, m]\}$ , where  $x_i^s$  represents the feature vector and  $y_i^s$  represents the label for the  $i$ -th sample in a source domain

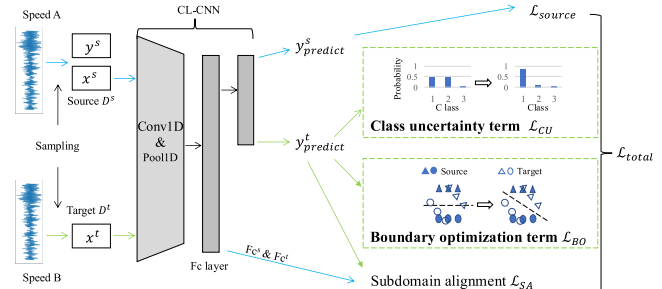


**Fig. 3:** The overall framework of our proposed SUO method. The class uncertainty term  $\mathcal{L}_{CU}$  quantifies the degree of classification ambiguity among samples, enabling the separation of target subdomains and facilitating the differentiation of high-similarity samples. The boundary optimization term  $\mathcal{L}_{BO}$  refines decision boundaries learned from the source domain to alleviate the adverse effects of boundary discrepancies between source and target domains. Additionally, the adjusted CL-CNN is adopted to achieve optimal cross-speed fault diagnosis under the supervision of total loss  $\mathcal{L}_{total}$ .

with  $m$  samples, and an unlabeled target domain  $D^t = \{x_i^t | i \in [1, n]\}$ , where  $x_i^t$  denotes the feature vector for the  $i$ -th sample in a target domain with  $n$  samples. The goal is to optimize the label classification function  $f(\cdot)$  by leveraging the knowledge from both the labeled source domain  $D^s$  and the unlabeled target domain  $D^t$ . Once optimized, the function  $f(\cdot)$  is used to classify the unlabeled samples in  $D^t$ , thereby facilitating fault diagnosis under different operating speeds.

### 2.2. Class Uncertainty

Samples with high similarity may exist within overlapping areas of multiple subdomains. This overlap leads to little probability differences between the subdomains for these samples, resulting in classification ambiguity. Such ambiguity poses substantial challenges for model classification, causing issues with class confusion.

To mitigate class confusion, it's important to increase the probability differences between subdomains, thus realizing the separation between subdomains. The class uncertainty term, denoted as  $\mathcal{L}_{CU}$ , is designed to quantify the degree of classification ambiguity among samples from the target domain. Minimizing  $\mathcal{L}_{CU}$  helps to achieve separation between target subdomains, making it easier to differentiate high-similarity samples. The calculation for  $\mathcal{L}_{CU}$  is as follows:

$$\mathcal{L}_{CU} = \sum_{i=1}^B \frac{1}{|C|} \sum_{j=1}^{|C|} \sum_{i \neq j} \left| \frac{y_j^T y_{\cdot i}}{\sum_{k=1}^{|C|} y_k^T y_{\cdot k}} \right|, \quad (1)$$

where  $\mathcal{L}_{CU}$  represents the class uncertainty value of target domain samples.  $B$  represents the batch size.  $|C|$  denotes the number of classes.  $y_j^T y_{\cdot i}$  measures the probabilities that samples are simultaneously classified into both class  $j$  and class  $i$ , and  $y_{\cdot j}$  denotes the probabilities of batch samples belonging to the  $j$ -th class.

### 2.3. Boundary Optimization

Although class uncertainty increases the probability differences between subdomains, the differing sample distributions between the source and target domains may render decision boundaries learned from the source domain unsuitable for the target domain.

To mitigate this problem, we introduce the boundary optimization term, denoted as  $\mathcal{L}_{BO}$ , which refines decision boundaries by

extracting boundary information from target domains. Minimizing  $\mathcal{L}_{BO}$  alleviates discrepancies in decision boundaries between source and target domains, improving the applicability of decision boundaries to both domains. The formula of  $\mathcal{L}_{BO}$  is as follows:

$$\mathcal{L}_{BO} = - \sum_{i=1}^n p^t(x_i^t) \log (q^t(x_i^t)), \quad (2)$$

where  $q^t(x_i^t)$  denotes the predicted distribution ( $y_{predict}^t$ ) for the  $i$ -th sample  $x_i^t$ .  $p^t(x_i^t)$  denotes the one-hot pseudo-label, which assigns the  $i$ -th sample the class with the highest probability of  $y_{predict}^t$ .

## 2.4. Model Training

Traditional subdomain alignment methods typically incorporate two primary components into their loss function: the cross-entropy term  $\mathcal{L}_{source}$ , which measures the discrepancy between predicted labels and the true labels in the source domain, and the subdomain alignment term  $\mathcal{L}_{SA}$ , which helps align the sample distributions between source and target subdomains.

The cross-entropy term  $\mathcal{L}_{source}$  is instrumental in extracting fault and decision boundary information from the source domain. The formula of  $\mathcal{L}_{source}$  is as follows:

$$\mathcal{L}_{source} = - \sum_{i=1}^m p^s(x_i^s) \log (q^s(x_i^s)), \quad (3)$$

where  $p^s(x_i^s)$  and  $q^s(x_i^s)$  represent the ground truth distribution and predicted distribution of the  $i$ -th sample  $x_i^s$ , respectively.

The subdomain alignment term, denoted as  $\mathcal{L}_{SA}$ , quantifies the discrepancy between the sample distributions from the source and target subdomains. To facilitate this measurement, unlabeled target samples are assigned pseudo-labels  $y_{pseudo}^t$  using the adjusted CL-CNN model [10], thereby generating the target domain samples  $D^t = \{x^t, y_{pseudo}^t\}$ . Subsequently, both the source domain samples  $D^s = \{x^s, y^s\}$  and the pseudo-labeled target domain samples  $D^t = \{x^t, y_{pseudo}^t\}$  are partitioned into  $C$  pairs of corresponding subdomains  $\{(S_i^s, S_i^t) \mid i \in [1, \dots, C]\}$ , where  $C$  represents the total number of classes.

Next, the sample distributions across all pairs of corresponding subdomains are aligned by minimizing  $\mathcal{L}_{SA}$ . The formulation of  $\mathcal{L}_{SA}$  is given by:

$$\mathcal{L}_{SA} = \frac{1}{C} \sum_{c=1}^C \sqrt{\left\| \frac{1}{m_c} \sum_{i=1}^{m_c} h(x_{ci}^s) - \frac{1}{n_c} \sum_{i=1}^{n_c} h(x_{ci}^t) \right\|_{\mathcal{H}}^2}, \quad (4)$$

where  $c$  denotes the  $c$ -th subdomain, and there are  $C$  subdomains in both the source and target domains. The function  $h(\cdot)$  is responsible for mapping feature representations of samples into the regenerative kernel Hilbert space  $\mathcal{H}$ . Specifically,  $h(x_{ci}^s)$  represents the mapping of the  $i$ -th feature representation  $F_{ci}^s$  from the source subdomain  $S_c^s$ , which contains  $m_c$  samples in total, while  $h(x_{ci}^t)$  represents the mapping of the  $i$ -th feature representation  $F_{ci}^t$  in the target subdomain  $S_c^t$ , which contains  $n_c$  samples.

To address class confusion issues during subdomain alignment, the overall loss  $\mathcal{L}_{total}$  integrates  $\mathcal{L}_{source}$  and  $\mathcal{L}_{SA}$  with additional components  $\mathcal{L}_{CU}$  and  $\mathcal{L}_{BO}$ . This comprehensive loss function is tailored to train the adjusted CL-CNN model for optimal cross-speed fault diagnosis. The total loss function  $\mathcal{L}_{total}$  is expressed as:

$$\mathcal{L}_{total} = \mathcal{L}_{source} + \alpha \mathcal{L}_{SA} + \gamma \mathcal{L}_{CU} + \beta \mathcal{L}_{BO}. \quad (5)$$

where  $\alpha$ ,  $\gamma$ , and  $\beta$  are hyper-parameters that weight the importance of the respective loss terms.

## 3. EXPERIMENTAL RESULTS AND ANALYSIS

### 3.1. Experiment Settings

**Datasets.** The proposed SUO method is evaluated using the CWRU and Jiangnan University (JNU) datasets, which comprise various types of data, including outer race fault, inner race fault, ball fault, and normal data[24, 25]. Specifically, for the CWRU dataset, the “12k Drive End Bearing Fault Data” is used, which features a sampling frequency of 12 kHz. This dataset comprises four sets of vibration data recorded at rotation speeds of 1797, 1772, 1750, and 1730 Revolutions Per Minute (RPM). Additionally, the JNU dataset, with a sampling frequency of 50 kHz, includes bearing vibration data recorded at rotational speeds of 600, 800, and 1000 RPM. Subsequently, the proportional periodic sampling strategy [10] is employed. This strategy involves constructing samples with a length of 420 for the CWRU dataset and 500 for the JNU dataset. All data from each operating speed in these datasets are used to construct ten or four types of samples, respectively. In this paper, the datasets, sample construction strategy, and resulting sample types and quantities are consistent with those outlined in reference [10].

**Cross-speed fault diagnosis tasks.** This paper describes the cross-speed fault diagnosis task as A→B, where the arrow starts from the source domain and ends in the target domain. There are six cross-speed fault diagnosis tasks for the JNU dataset, namely, 600→800, 600→1000, 800→600, 800→1000, 1000→600 and 1000→800. Additionally, there are twelve cross-speed tasks for the CWRU dataset, namely, 1797→1772, 1797→1750, 1797→1730, 1772→1797, 1772→1750, 1772→1730, 1750→1797, 1750→1772, 1750→1730, 1730→1797, 1730→1772, 1730→1750.

**Parameter setup.** All experiments are conducted five times to mitigate the interference of randomness. The target domain samples are divided into a training set and a testing set with a ratio of [0.9, 0.1]. All experiments are performed on a desktop computer equipped with an “Intel(R) Core(TM) i5-8600K CPU @ 3.60GHz” and an “NVIDIA GeForce GTX 1080 Ti” graphics card. The deep learning framework employed is Pytorch 1.9.0. Following some weight tuning experiments, the hyper-parameters are set to  $\alpha = 0.5$ ,  $\gamma = 0.5$ , and  $\beta = 0.7$ . Training parameters include 80 epochs, a batch size of 32, a learning rate of 0.001, and a 1D convolutional layer with a kernel size of 21 and a stride of 1.

**Method settings.** To validate the efficacy of the proposed SUO method, we perform a comparative analysis against five recent methods: JMMD [26], MK-MMD [26], TCTL [10], JSAN [27], and DSAFGCN [28]. Additionally, we performed an ablation study involving three variants of our method to assess the contribution of loss terms  $\mathcal{L}_{CU}$  and  $\mathcal{L}_{BO}$ . Three ablation methods are defined as follows: **A1** excludes the loss terms  $\mathcal{L}_{CU}$  and  $\mathcal{L}_{BO}$  from the SUO method; **A2** excludes the loss term  $\mathcal{L}_{CU}$  from the SUO method; **A3** excludes the loss term  $\mathcal{L}_{BO}$  from the SUO method.

### 3.2. Comparative Analysis of Overall Performance

To evaluate the overall effectiveness of our proposed SUO method, we perform a comparative analysis against five recent methods. The results, encompassing 18 cross-speed fault diagnosis tasks, are summarized in Table 1. Our SUO method achieves the highest average accuracy of 99.86% with the lowest standard deviation (SD) of 0.21, outperforming JMMD, MK-MMD, TCTL, JSAN, and DSAFGCN. Specifically, SUO improves average accuracy by 1.18%, 2.61%, 0.46%, 1.57%, and 0.93% over these methods, respectively. Additionally, SUO shows a notable advantage in the cross-speed fault diagnosis tasks 1730→1797 and 1000→600.

**Table 1:** The overall performance of SUO compared with five recent methods.

Method	JMMD	MK-MMD	TCTL	JSAN	DSAGCN	Our SUO
1797→1772	<b>100</b>	98.51	99.61	99.84	99.64	99.97
1797→1750	99.61	99.74	99.59	<b>100</b>	<b>100</b>	<b>100</b>
1797→1730	99.68	93.72	99.85	<b>100</b>	99.36	<b>100</b>
1772→1797	98.54	93.33	98.83	99.81	<b>100</b>	99.46
1772→1750	<b>100</b>	<b>100</b>	99.59	<b>100</b>	<b>100</b>	<b>100</b>
1772→1730	<b>100</b>	99.94	99.86	99.84	<b>100</b>	<b>100</b>
1750→1797	<b>99.62</b>	93.72	99.51	99.43	99.13	99.58
1750→1772	99.74	99.61	99.66	99.84	99.24	<b>99.95</b>
1750→1730	<b>100</b>	<b>100</b>	99.86	<b>100</b>	<b>100</b>	<b>100</b>
1730→1797	98.85	92.18	97.83	98.47	99.34	<b>99.87</b>
1730→1772	99.09	99.09	99.15	97.08	99.03	<b>99.95</b>
1730→1750	<b>100</b>	<b>100</b>	99.59	99.84	<b>100</b>	<b>100</b>
600→800	97.95	98.33	99.18	97.76	98.67	<b>99.92</b>
600→1000	97.27	97.2	98.93	95.56	97.84	<b>99.87</b>
800→600	96.59	96.21	99.51	93.17	97.16	<b>99.30</b>
800→1000	99.11	99.1	99.75	98.98	99.02	<b>100</b>
1000→600	91.78	91.98	99.07	90.59	93.69	<b>99.65</b>
1000→800	98.46	97.78	99.88	99.06	98.53	<b>99.88</b>
Average	98.68	97.25	99.40	98.29	98.93	<b>99.86</b>
SD	1.99	2.93	0.51	2.66	1.53	<b>0.21</b>

These performance gains are attributed to the limitations of existing methods, which predominantly focus on aligning sample distributions between source and target domains through global or sub-domain correlations. These methods often neglect essential relationships such as high sample similarity between target subdomains and the discrepancies in decision boundaries between source and target domains, leading to significant class confusion issues. In contrast, as illustrated in Figure 1 (b), SUO effectively addresses class confusion by incorporating the class uncertainty term, which accounts for high sample similarity between target subdomains, alongside a boundary optimization term that alleviates discrepancies in decision boundaries between source and target domains.

### 3.3. Comparative Analysis between Ablation Methods

To demonstrate the impact of the terms  $\mathcal{L}_{CU}$  and  $\mathcal{L}_{BO}$ , we compare the SUO method with three ablation methods using the CWRU and JNU datasets. The results, including average accuracy and standard deviation (SD) across 18 cross-speed fault diagnosis tasks, are summarized in Table 2.

As illustrated in Table 2, the removal of either one or both terms results in performance degradation for the A1, A2, and A3 methods when compared to our SUO method. Specifically, the average accuracy decreases by 2.77%, 0.84%, and 3.99%, respectively, while the SD increases by 7.92%, 7%, and 13.3%, respectively. Notably, in the cross-speed task 1797→1750, the average accuracies of the three ablation methods A1, A2, and A3 are 67.14%, 86.19%, and 72.38%, respectively, which are markedly lower than the 100% accuracy achieved by our SUO method. These results underscore the critical role of the class uncertainty ( $\mathcal{L}_{CU}$ ) and boundary optimization ( $\mathcal{L}_{BO}$ ) terms. We attribute these findings to the simultaneous integration of the class uncertainty and boundary optimization terms, which can address the class confusion issues more comprehensively, thereby achieving optimal diagnostic performance.

### 3.4. Sensitivity Analysis of Parameters

In this section, we examine how the weights  $\alpha$ ,  $\beta$ , and  $\gamma$  affect the average accuracy of our diagnostic model, assuming that each parameter influences the model independently of the others. We employ a one-at-a-time (OAT) sensitivity analysis to examine how variations in these parameters affect the SUO method's performance on the cross-speed task 800→1000. For simplicity, we restrict the range of each parameter to (0, 1: 0.1].

**Table 2:** Results of ablation experiments.

Method	A1	A2	A3	Our SUO
1797→1772	<b>100</b>	<b>100</b>	86.20	99.97
1797→1750	67.14	86.19	72.38	<b>100</b>
1797→1730	86.21	<b>100</b>	72.31	<b>100</b>
1772→1797	98.34	99.23	<b>99.87</b>	99.46
1772→1750	<b>100</b>	<b>100</b>	99.78	<b>100</b>
1772→1730	<b>100</b>	<b>100</b>	97.54	<b>100</b>
1750→1797	99.94	99.81	<b>100</b>	99.58
1750→1772	<b>100</b>	<b>100</b>	99.95	99.95
1750→1730	<b>100</b>	<b>100</b>	<b>100</b>	<b>100</b>
1730→1797	99.90	99.78	<b>99.97</b>	99.87
1730→1772	98.4	99.97	<b>100</b>	99.95
1730→1750	<b>100</b>	99.97	<b>100</b>	<b>100</b>
600→800	99.88	99.30	99.83	<b>99.92</b>
600→1000	99.43	99.51	99.68	<b>99.87</b>
800→600	<b>99.70</b>	99.25	99.67	99.30
800→1000	99.77	99.87	99.46	<b>100.00</b>
1000→600	99.23	99.66	99.06	<b>99.65</b>
1000→800	99.65	99.82	<b>99.90</b>	99.88
Average	97.09	99.02	95.87	<b>99.86</b>
SD	8.13	7.21	13.51	<b>0.21</b>

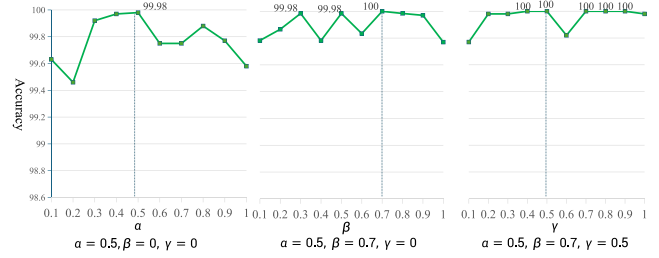


**Fig. 4:** Sensitivity analysis of parameters, and  $\alpha = 0.5$ ,  $\beta = 0.7$  and  $\gamma = 0.5$  are selected in this paper.  $\alpha$ ,  $\gamma$ , and  $\beta$  are weight parameters that control the contributions of the subdomain alignment term, class uncertainty term, and boundary optimization term, respectively.

Initially, we set  $\beta = \gamma = 0$  to investigate the impact of  $\alpha$  on the diagnostic accuracy of the SUO method. As illustrated in Figure 3 (left), SUO achieves its peak accuracy of 99.98% when  $\alpha = 0.5$ . Subsequently, with  $\alpha = 0.5$  and  $\gamma = 0$ , we analyze the influence of  $\beta$  on diagnostic accuracy, as depicted in Figure 3 (middle). The model attains 100% accuracy at  $\beta = 0.7$ , which we designate as the optimal value for  $\beta$ . Following this, with  $\alpha = 0.5$  and  $\beta = 0.7$ , we evaluate the effect of  $\gamma$  on diagnostic accuracy, as illustrated in Figure 3 (right). The accuracy reaches its maximum value of 100% for  $\gamma$  values of 0.4, 0.5, 0.7, 0.8, or 0.9. For simplicity, we assume equal importance for  $\gamma$  and  $\alpha$ , setting both to  $\gamma = \alpha = 0.5$ . Consequently, this paper defines  $\alpha = 0.5$ ,  $\gamma = 0.5$ , and  $\beta = 0.7$  as the hyper-parameters to obtain the optimal diagnostic accuracy.

## 4. CONCLUSION

In this paper, we attribute the limited performance of existing domain or subdomain alignment methods for cross-speed bearing fault diagnosis to class confusion issues. To address this, we propose the subdomain uncertainty optimization method that incorporates class uncertainty to differentiate high-similarity samples from target domains better and employs boundary optimization to alleviate decision boundary discrepancies between source and target domains. Moreover, this method adjusts the CL-CNN network to collaborate with the class uncertainty and boundary optimization for optimal cross-speed fault diagnosis. Comprehensive experiments conducted across 18 cross-speed tasks validate the effectiveness of our method, which achieves a stable average accuracy of 99.86%.

## 5. REFERENCES

- [1] Zuozhou Pan, Zhiping Lin, YuanJin Zheng, and Zong Meng, “Fast fault diagnosis method of rolling bearings in multi-sensor measurement enviroment,” in *ICASSP 2022-2022 IEEE International Conference on Acoustics, Speech and Signal Processing (ICASSP)*, 2022.
- [2] Hasan Ocak and Kenneth A Loparo, “A new bearing fault detection and diagnosis scheme based on hidden markov modeling of vibration signals,” in *2001 IEEE International Conference on Acoustics, Speech, and Signal Processing. Proceedings (Cat. No. 01CH37221)*, 2001.
- [3] Hua Li, Tao Liu, Xing Wu, and Qing Chen, “An optimized vmd method and its applications in bearing fault diagnosis,” *Measurement*, 2020.
- [4] Xiaohan Chen, Rui Yang, Yihao Xue, Mengjie Huang, Roberto Ferrero, and Zidong Wang, “Deep transfer learning for bearing fault diagnosis: A systematic review since 2016,” *IEEE Transactions on Instrumentation and Measurement*, 2023.
- [5] Yifan Li, Xin Zhang, Zaigang Chen, Yaocheng Yang, Changqing Geng, and Ming J Zuo, “Time-frequency ridge estimation: An effective tool for gear and bearing fault diagnosis at time-varying speeds,” *Mechanical Systems and Signal Processing*, 2023.
- [6] Gregory W Vogl, Brian A Weiss, and Moneer Helu, “A review of diagnostic and prognostic capabilities and best practices for manufacturing,” *Journal of Intelligent Manufacturing*, 2019.
- [7] Liang Guo, Yaguo Lei, Saibo Xing, Tao Yan, and Naipeng Li, “Deep convolutional transfer learning network: A new method for intelligent fault diagnosis of machines with unlabeled data,” *IEEE Transactions on Industrial Electronics*, 2018.
- [8] Baoye Song, Yiyuan Liu, Jingzhong Fang, Weibo Liu, Maiying Zhong, and Xiaohui Liu, “An optimized cnn-bilstm network for bearing fault diagnosis under multiple working conditions with limited training samples,” *Neurocomputing*, 2024.
- [9] Sixiang Jia, Yongbo Li, Xinyue Wang, Dingyi Sun, and Zichen Deng, “Deep causal factorization network: A novel domain generalization method for cross-machine bearing fault diagnosis,” *Mechanical Systems and Signal Processing*, 2023.
- [10] Jianbo Zheng, Bin Jiang, and Chao Yang, “Proportional periodic sampling for cross-load bearing fault diagnosis,” *International Journal of Machine Learning and Cybernetics*, 2024.
- [11] Yaguo Lei, Bin Yang, Xinwei Jiang, Feng Jia, Naipeng Li, and Asoke K Nandi, “Applications of machine learning to machine fault diagnosis: A review and roadmap,” *Mechanical Systems and Signal Processing*, 2020.
- [12] Yaowei Shi, Aidong Deng, Minqiang Deng, Meng Xu, Yang Liu, Xue Ding, and Jing Li, “Transferable adaptive channel attention module for unsupervised cross-domain fault diagnosis,” *Reliability Engineering & System Safety*, 2022.
- [13] Songjun Han and Zhipeng Feng, “Intelligent fault diagnosis of planetary gearboxes under time-varying conditions based on dynamic adversarial balance adaptation with multi-label information confusion,” *Measurement Science and Technology*, 2023.
- [14] Karsten M Borgwardt, Arthur Gretton, Malte J Rasch, Hans-Peter Kriegel, Bernhard Schölkopf, and Alex J Smola, “Integrating structured biological data by kernel maximum mean discrepancy,” *Bioinformatics*, 2006.
- [15] Arthur Gretton, Dino Sejdinovic, Heiko Strathmann, Sivaraman Balakrishnan, Massimiliano Pontil, Kenji Fukumizu, and Bharath K Sriperumbudur, “Optimal kernel choice for large-scale two-sample tests,” *Advances in neural information processing systems*, 2012.
- [16] Mingsheng Long, Han Zhu, Jianmin Wang, and Michael I Jordan, “Deep transfer learning with joint adaptation networks,” in *International conference on machine learning*, 2017.
- [17] Baochen Sun and Kate Saenko, “Deep coral: Correlation alignment for deep domain adaptation,” in *Computer Vision–ECCV 2016 Workshops: Amsterdam, The Netherlands, October 8–10 and 15–16, 2016, Proceedings, Part III 14*, 2016.
- [18] Pengfei Chen, Rongzhen Zhao, Tianjing He, Kongyuan Wei, and Qidong Yang, “Unsupervised domain adaptation of bearing fault diagnosis based on joint sliced wasserstein distance,” *ISA transactions*, 2022.
- [19] Yongchun Zhu, Fuzhen Zhuang, Jindong Wang, Guolin Ke, Jingwu Chen, Jiang Bian, Hui Xiong, and Qing He, “Deep subdomain adaptation network for image classification,” *IEEE transactions on neural networks and learning systems*, 2020.
- [20] Quan Qian, Yi Qin, Jun Luo, and Dengyu Xiao, “Cross-machine transfer fault diagnosis by ensemble weighting subdomain adaptation network,” *IEEE Transactions on Industrial Electronics*, 2023.
- [21] Zuoyi Chen, Jun Wu, Chao Deng, Chao Wang, and Yuanhang Wang, “Residual deep subdomain adaptation network: A new method for intelligent fault diagnosis of bearings across multiple domains,” *Mechanism and Machine Theory*, 2022.
- [22] Ying Jin, Ximei Wang, Mingsheng Long, and Jianmin Wang, “Minimum class confusion for versatile domain adaptation,” in *Computer Vision–ECCV 2020: 16th European Conference, Glasgow, UK, August 23–28, 2020, Proceedings, Part XXI 16*, 2020.
- [23] Qing Zhang, Lv Tang, Jianping Xuan, Tielin Shi, and Rui Li, “An uncertainty relevance metric-based domain adaptation fault diagnosis method to overcome class relevance caused confusion,” *Reliability Engineering & System Safety*, 2023.
- [24] Wade A Smith and Robert B Randall, “Rolling element bearing diagnostics using the case western reserve university data: A benchmark study,” *Mechanical systems and signal processing*, 2015.
- [25] Ke Li, Xueliang Ping, Huaiqing Wang, Peng Chen, and Yi Cao, “Sequential fuzzy diagnosis method for motor roller bearing in variable operating conditions based on vibration analysis,” *Sensors*, 2013.
- [26] Zhibin Zhao, Qiyang Zhang, Xiaolei Yu, Chuang Sun, Shibin Wang, Ruqiang Yan, and Xuefeng Chen, “Applications of unsupervised deep transfer learning to intelligent fault diagnosis: A survey and comparative study,” *IEEE Transactions on Instrumentation and Measurement*, 2021.
- [27] Baoqiang Wang, Yuan Wei, Shulin Liu, Dongfang Zhao, and Xiaoyang Liu, “Unsupervised joint subdomain adaptation network for fault diagnosis,” *IEEE Sensors Journal*, 2022.
- [28] Mohammadreza Ghorvei, Mohammadreza Kavianpour, Mohammad TH Beheshti, and Amin Ramezani, “Spatial graph convolutional neural network via structured subdomain adaptation and domain adversarial learning for bearing fault diagnosis,” *Neurocomputing*, 2023.